

# How Dynamics Improve Fault Detection: A Gaussian LTI Case

Xinrui Gao\*, Anbang Hu\*, Yuri A.W. Shardt\*

\* *Department of Automation Engineering, Technical University of Ilmenau, Ilmenau, Thuringia, Germany, 98684*  
(e-mail: {xinrui.gao, [yuri.shardt@tu-ilmenau.de](mailto:yuri.shardt@tu-ilmenau.de), [huanbang1995@gmail.com](mailto:huanbang1995@gmail.com))

---

**Abstract:** Fault detection has witnessed a rapid development and many approaches have been proposed in recent decades. However, many of them are based on heuristic solutions that do not check the applicability and optimality of the resulting fault-detection systems. This paper starts from a hypothesis test that subsumes all fault-detection problems, based on which a unified optimisation problem is formulated. The resulting optimal solution defines the deemed-normal region of the system. It is proven that dynamic information shrinks the deemed-normal region and improves detection performance in Gaussian LTI systems. The theoretical results are verified on a simulated three-tank system. Compared with the static method, the fault-detection rate (FDR) of the dynamic method based on a Kalman filter increases from 96% and 56% to 99% and 100% for two faults, respectively, while the false-alarm rate (FAR) decreases from 7.38% and 0.88% to 0.75% and 0.63%. This paper provides a theoretical foundation for understanding fault detection for Gaussian LTI systems, and avoids using any heuristic proposals and solutions for the problem of fault detection. The rigorous justification of the well-known fact that incorporating dynamic information improves fault-detection performance implies a roadmap towards advanced methods for more complex cases. In addition, the analysis including the idea of a deemed-normal region has the potential to be extended to a physically meaningful framework for performance assessment of fault diagnosis and fault-tolerant control systems.

*Keywords:* fault diagnosis, deemed-normal region, Kalman filter, three-tank system.

---

## 1. INTRODUCTION

The problem of fault detection and isolation has been extensively studied in recent decades. Based on the idea of analytical redundancy, the task of fault detection involves the generation and evaluation of residuals (Ding, 2013). Generation of residuals seeks to generate diagnostic residual signals that possess desired properties, *e.g.*, are sensitive to specific faults, are robust to disturbances, and exploit specific system characteristics as much as possible. Evaluation of the residuals refers to designing some evaluation functions for the resulting residual signals to make decisions regarding whether the system is normal or not. The pioneering work of Beard (1971) and Jones (1973) marked the beginning of observer-based residual generation, which led to great development in the area (Bernardi & Adam, 2020). The parity-space approach is another important type of residual-generation method (Song, et al., 2020). In addition, data-driven fault detection (Md Nor, Che Hassan, & Hussain, 2020) using data analytics and machine learning has drawn attention, *e.g.*, principal component analysis (Wise, et al., 1990), independent component analysis (Lee, et al., 2006), slow-feature analysis (Gao & Shardt, 2021), and neural networks (Gao, Yang, & Feng, 2020). Compared to the generation of residuals, the evaluation methods have received less attention. Common choices for evaluation functions include the  $l_2$ -norm (Shang, et al., 2021), the Mahalanobis distance, and the Kullback-Leibler (KL) divergence (Harmouche, et al., 2014).

Many fault detection approaches have the following disadvantages. First, the generation and evaluation of residuals are two separate steps when designing fault-detection systems. This means that, despite each of the individual components being optimal, the overall system may not necessarily be optimal. Second, as mentioned in Ding (2021), many data-driven methods are a mechanical combination of machine learning and statistical decision methods, which may not work together. Third, some optimal fault-detection problems are formulated heuristically, without indicating in which sense it is optimal and how the performance is improved. For instance, some methods maximise the Frobenius norm or the pseudodeterminant of a parameter matrix (Shang, et al., 2021), while some minimise the alarm threshold (Esfahani & Lygeros, 2015). These methods do not indicate how the heuristic proposals are related to the optimal performance of fault detection. Finally, many fault-detection methods use an evaluation function without checking its applicability and optimality.

Thus, this paper proposes a solution that avoids all heuristic proposals and solutions. Starting from hypothesis testing, the foundation for all fault-detection problems, fault detection is formulated as a unified optimisation problem that possesses clear physical meaning. With specific assumptions on the residual signals, the unified optimisation problem gives an optimal solution for fault detection, which is the generalised likelihood ratio test (GLRT) statistic. Finally, for Gaussian linear time-invariant (LTI) systems, it is proven that incorporation of system dynamics shrinks the deemed-normal

region defined by the optimal solution, and improves fault-detection performance. As well, the proposed theoretical results are tested on a three-tank system.

## 2. A UNIFIED FORMULATION FOR OPTIMAL FAULT DETECTION

Starting from a general hypothesis test that subsumes all fault-detection problems, this section introduces a unified optimisation problem for fault detection.

### 2.1 Fault Detection and Performance Assessment

Suppose that  $\mathbf{f} \in \mathbb{R}^{n_f}$  with a dimension of  $n_f$  is the fault to be detected, and the system affected by  $\mathbf{f}$  satisfies

$$\mathbf{f} = 0 : \text{fault-free}; \mathbf{f} \neq 0 : \text{faulty} \quad (1)$$

Fault detection is essentially a problem to find an evaluation function  $J(\cdot): \mathbb{R}^{n_y} \rightarrow \mathbb{R}_+$  and its threshold  $J_{th}$  such that

$$\begin{cases} J(\mathbf{y}|\mathbf{f} \neq 0) > J_{th} \rightarrow \text{alarm} \\ J(\mathbf{y}|\mathbf{f} = 0) \leq J_{th} \rightarrow \text{no alarm} \end{cases} \quad (2)$$

where  $\mathbf{y} \in \mathbb{R}^{n_y}$  is the measurement with a dimension of  $n_y$ .

In a probabilistic setting, fault detection based on decision logic (2) is actually a hypothesis test with ‘‘fault-free’’ being the null hypothesis and ‘‘faulty’’ the alternative hypothesis. Due to mismatch between a model and the real system, as well as inevitable disturbances, the hypothesis testing could have false positives (*i.e.*, Type I error or  $\alpha$ -error) and false negatives (*i.e.*, Type II error or  $\beta$ -error). In the fault-detection problem, false positives are the false-alarm rate (FAR)

$$\text{FAR} = \Pr\{J(\mathbf{y}) > J_{th} | \mathbf{f} = 0\} = \alpha \quad (3)$$

while false negatives are the misdetection rate (MDR)

$$\text{MDR} = \Pr\{J(\mathbf{y}) \leq J_{th} | \mathbf{f} \neq 0\} = \beta \quad (4)$$

MDR is complementary with the fault-detection rate (FDR)

$$\text{FDR} = \Pr\{J(\mathbf{y}) > J_{th} | \mathbf{f} \neq 0\} = 1 - \beta \quad (5)$$

It is clear from the logic (2) that designing fault-detection systems is a trade-off between FAR and FDR/MDR. It is impossible for any trivial method to improve both of them (Shardt, 2022), *e.g.*, increasing the threshold will result in a lower FAR at the cost of decreasing FDR. Using FAR and FDR concurrently, fault detection is comprehensively formulated as an optimisation problem (Ding, 2021)

$$\{J, J_{th}\} = \arg \max_{J, J_{th}, \text{FAR} \leq \alpha} \text{FDR} \quad (6)$$

This general formulation gives a unified solution for optimal fault detection in the sense of maximising FDR while keeping FAR within a tolerance  $\alpha$ .

### 2.2 Generation of Residuals and Optimal Fault Detection

If the tolerance for false positives is zero, that is,  $\alpha = 0$ , the fault-detection logic (2) yields

$$J_{th} = \sup J(\mathbf{y} | \mathbf{f} = 0) \quad (7)$$

Supposing that the fault and noise are both additive, then measurement  $\mathbf{y}$  can be decomposed into contributions  $\mathbf{y}_n$ ,  $\mathbf{y}_d$ , and  $\mathbf{y}_f$  from the nominal value, disturbance, and fault, respectively, namely  $\mathbf{y} = \mathbf{y}_n + \mathbf{y}_d + \mathbf{y}_f$ . Recalling that  $J$  is positive semidefinite by definition in (2), it follows that

$$J(\mathbf{y}) \geq J(\mathbf{y}_f) - J(\mathbf{y}_n + \mathbf{y}_d) \geq J(\mathbf{y}_f) - \sup J(\mathbf{y} | \mathbf{f} = 0) \quad (8)$$

To ensure that a fault is sufficiently detected, it requires

$$J(\mathbf{y}) \geq J(\mathbf{y}_f) - \sup J(\mathbf{y} | \mathbf{f} = 0) > J_{th} \quad (9)$$

which, recalling (7), gives (Frank & Ding, 1997)

$$J(\mathbf{y}_f) > 2 \sup J(\mathbf{y} | \mathbf{f} = 0) = 2 \sup J(\mathbf{y}_n + \mathbf{y}_d) \quad (10)$$

Equation (10) gives the sufficient detectability of a fault  $\mathbf{f}$ . It is clear that the nominal contribution  $\mathbf{y}_n$  will weaken the sufficient detectability, since with it,  $J(\mathbf{y})$  will be larger. If the nominal contribution  $J(\mathbf{y}_n)$  is large, those faults with small contribution  $J(\mathbf{y}_f)$  might not be detectable.

To eliminate this nominal effect, instead of measurements  $\mathbf{y}$ , the residual between the measurement and its nominal estimate is used for fault detection, that is,

$$\mathbf{r} = \mathbf{y} - \hat{\mathbf{y}} = \mathbf{y} - \mathbb{E}_{p(d)}(\mathbf{y}_n + \mathbf{y}_d) = \mathbf{y}_d + \mathbf{y}_f \quad (11)$$

where the nominal estimate is  $\hat{\mathbf{y}} = \mathbb{E}_{p(d)}(\mathbf{y}_n + \mathbf{y}_d) = \mathbf{y}_n$ , as the distribution of disturbance is assumed to be symmetric. Equation (11) is the residual generator, which involves estimating the nominal conditions, computing the difference, and sometimes postprocessing, *e.g.*, filtering (Ding, 2013).

Ideally, the residual generated using (11) should be zero in the fault-free case and should equal the fault contribution in the faulty case, that is,

$$\mathbf{y}_d = 0; \mathbf{y}_f = 0 \text{ if } \mathbf{f} = 0; \mathbf{y}_f \neq 0 \text{ if } \mathbf{f} \neq 0 \quad (12)$$

Equation (12) is called perfect unknown-input decoupling (PUIDP) (Ding, 2013). If the PUIDP condition holds, every fault  $\mathbf{f} \neq 0$  will be perfectly detected. However, in the case that PUIDP is impossible, designing fault-detection methods will inevitably lead to a trade-off between FDR and FAR. This demands a unified formulation for optimal fault detection. Rewriting Problem (6) using the residual generated by (11) gives the optimal solution for fault detection, that is,

$$\{J, J_{th}\} = \arg \max_{J, J_{th}, \Pr\{J(\mathbf{r}) > J_{th} | \mathbf{f} = 0\} \leq \alpha} \Pr\{J(\mathbf{r}) > J_{th} | \mathbf{f} \neq 0\} \quad (13)$$

## 3. IMPROVING FAULT DETECTION USING SYSTEM DYNAMICS

Having introduced the optimal fault-detection problem based on residual generators, this section will show how incorporating system dynamics in the generation of residuals improves fault detection for Gaussian LTI systems.

### 3.1 Optimal Fault Detection for Gaussian Systems

For Gaussian systems, the residual (11) can be represented as

$$\mathbf{r} = \boldsymbol{\varepsilon} + \mathbf{E}\mathbf{f} = \boldsymbol{\varepsilon} + \bar{\mathbf{f}}, \boldsymbol{\varepsilon} \sim \mathcal{N}(0, \boldsymbol{\Sigma}) \quad (14)$$

where the white noise  $\boldsymbol{\varepsilon}$  equals the  $\mathbf{y}_d$ ,  $\mathbf{f} \notin \text{null}(\mathbf{E})$  is the deterministic fault, and  $\mathbf{E}$  maps  $\mathbf{f}$  to the fault contribution  $\mathbf{y}_f$ . Note that FDR and FAR can be regarded as the likelihood of triggering alarms in faulty and fault-free cases, respectively. With the explicit representation (14) of residuals, Problem (13) is rewritten as (Gao, Xie, & Shardt, 2023)

$$\begin{aligned} \max R &= \log \frac{\text{FDR}}{\text{FAR}} = \log \frac{L(\mathbf{r}|\mathbf{f} \neq 0)}{L(\mathbf{r}|\mathbf{f} = 0)} \\ &= \frac{1}{2} \left( \mathbf{r}^\top \boldsymbol{\Sigma}^{-1} \mathbf{r} - (\mathbf{r} - \bar{\mathbf{f}})^\top \boldsymbol{\Sigma}^{-1} (\mathbf{r} - \bar{\mathbf{f}}) \right) \end{aligned} \quad (15)$$

where  $L$  is the Gaussian likelihood function of the system being identified as faulty. Since  $\boldsymbol{\Sigma}$  is non-negative definite, omitting the constant  $\frac{1}{2}$ , the maximum of  $R$  in (15) gives the optimal solution for fault detection, that is

$$J = R^* = \mathbf{r}^\top \boldsymbol{\Sigma}^{-1} \mathbf{r}, J(\mathbf{r}|\mathbf{f} = 0) \leq J_{th} = \chi^2(m, \alpha) \quad (16)$$

where  $m$  is the degrees of freedom of the  $\chi^2$ -distribution. It should be noted that the threshold  $J_{th}$  is the  $\alpha$ -quantile of a  $\chi^2$ -distribution corresponding to the fault-free case, *i.e.*,  $\Pr\{J \geq J_{th} | \mathbf{f} = 0\} = \alpha$ . During the design of fault-detection strategies, the boundary of the normal region is defined, and any point outside the boundary will be considered as faulty.

Solution (16) is the well-known GLRT statistic (Gustafsson, 2000). Geometrically, it defines an ellipsoid whose lengths of the semi-axes are proportional to singular values of  $\boldsymbol{\Sigma}$ . This ellipsoid contains a region that is considered to be normal with a confidence  $1 - \alpha$  based on corresponding detection methods. Hence, we call the region inside the ellipsoid the *deemed-normal region*. We will see how incorporating system dynamics in residual generation shrinks the deemed-normal region defined by (16), and improves fault detection.

### 3.2 Generation of Residuals Based on the Kalman Filter

Consider a discrete LTI system

$$\begin{cases} \mathbf{x}(t+1) = \mathbf{A}\mathbf{x}(t) + \mathbf{B}\mathbf{u}(t) + \boldsymbol{\omega}(t) \\ \mathbf{y}(t) = \mathbf{C}\mathbf{x}(t) + \mathbf{D}\mathbf{u}(t) + \mathbf{v}(t) \end{cases} \quad (17)$$

where  $\mathbf{x} \in \mathbb{R}^{n_x}$ ,  $\mathbf{u} \in \mathbb{R}^{n_u}$ , and  $\mathbf{y} \in \mathbb{R}^{n_y}$  are the system state, input, and output vectors, respectively, and matrices  $\mathbf{A}$ ,  $\mathbf{B}$ ,  $\mathbf{C}$ , and  $\mathbf{D}$  are of proper dimensions. Process and measurement noise  $\boldsymbol{\omega}(t)$  and  $\mathbf{v}(t)$  are independent of  $\mathbf{x}$  and  $\mathbf{u}$ , and

$$\boldsymbol{\omega}(t) \sim \mathcal{N}(0, \boldsymbol{\Sigma}_\omega(t)), \mathbf{v}(t) \sim \mathcal{N}(0, \boldsymbol{\Sigma}_v(t))$$

$$\mathbb{E} \left( \begin{bmatrix} \boldsymbol{\omega}(i) \\ \mathbf{v}(i) \end{bmatrix} \begin{bmatrix} \boldsymbol{\omega}(j) \\ \mathbf{v}(j) \end{bmatrix}^\top \right) = \begin{bmatrix} \boldsymbol{\Sigma}_\omega(i) & 0 \\ 0 & \boldsymbol{\Sigma}_v(i) \end{bmatrix} \delta_{i,j}, \delta_{i,j} = \begin{cases} 1, i = j \\ 0, i \neq j \end{cases}$$

In the spirit of (11), the residual generator for the system (17) is implemented as

$$\mathbf{r}(t) = \mathbf{y}(t) - \hat{\mathbf{y}}(t) \quad (18)$$

where the nominal estimate  $\hat{\mathbf{y}}(t)$  can be obtained by the recursive algorithm of the Kalman filter (Khodarahmi & Maihami, 2023)

$$\begin{aligned} \hat{\mathbf{y}}(t) &= \mathbf{C}\hat{\mathbf{x}}(t) + \mathbf{D}\mathbf{u}(t) \\ \hat{\mathbf{x}}(t) &= \mathbf{A}\hat{\mathbf{x}}(t-1) + \mathbf{B}\mathbf{u}(t-1) + \mathbf{K}(t-1)\mathbf{r}(t-1) \\ \hat{\mathbf{x}}(0) &= \mathbf{x}(0) \end{aligned} \quad (19)$$

with the Kalman filter gain  $\mathbf{K}$  at time  $t$

$$\mathbf{K}(t) = \mathbf{P}(t|t-1)\mathbf{C}^\top (\mathbf{C}\mathbf{P}(t|t-1)\mathbf{C}^\top + \boldsymbol{\Sigma}_v(t))^{-1} \quad (20)$$

and the covariance matrix  $\mathbf{P}(t|t-1)$  of the error of one-step-ahead state prediction

$$\begin{aligned} \mathbf{P}(t|t-1) &= \text{Cov}(\mathbf{x}(t) - \mathbf{A}\hat{\mathbf{x}}(t-1)) \\ &= \mathbf{A}\mathbf{P}(t-1)\mathbf{A}^\top + \boldsymbol{\Sigma}_\omega(t-1) \end{aligned} \quad (21)$$

and  $\mathbf{P}(t-1)$  is covariance matrix of the error of the state estimate at time  $t-1$ , that is,

$$\mathbf{P}(t) = \text{Cov}(\mathbf{x}(t) - \hat{\mathbf{x}}(t)) = (\mathbf{I} - \mathbf{K}(t)\mathbf{C})\mathbf{P}(t|t-1) \quad (22)$$

Equations (18) to (22) describe Kalman-filter-based residual generation for dynamic system (17). Since residuals resulting from Kalman filters are white, residual (18) is equivalent to (14), thereby satisfying the optimal solution (16).

### 3.3 Shrinking the Uncertainty of Residuals Using Dynamics

Using a lemma and a theorem, this subsection will show how dynamic information shrinks the deemed-normal region.

**Lemma 1:** *Given the dynamic system (17), the Kalman filter given by (19) to (22) decomposes the variance of the system outputs into contributions from the state-estimate error, the state estimate, and the measurement noise, that is,*

$$\boldsymbol{\Sigma}_y(t) = \mathbf{C}\mathbf{P}(t)\mathbf{C}^\top + \mathbf{C}\boldsymbol{\Sigma}_x(t)\mathbf{C}^\top + \boldsymbol{\Sigma}_v(t) \quad (23)$$

**Proof:** The variance of the system outputs is

$$\begin{aligned} \boldsymbol{\Sigma}_y(t) &= \mathbb{E}(\mathbf{y}(t)\mathbf{y}(t)^\top) - \mathbb{E}(\mathbf{y}(t))\mathbb{E}(\mathbf{y}(t))^\top \\ &= \mathbf{C} \left( \mathbb{E}(\mathbf{x}(t)\mathbf{x}(t)^\top) - \mathbb{E}(\mathbf{x}(t))\mathbb{E}(\mathbf{x}(t))^\top \right) \mathbf{C}^\top + \boldsymbol{\Sigma}_v(t) \\ &= \mathbf{C}\boldsymbol{\Sigma}_x(t)\mathbf{C}^\top + \boldsymbol{\Sigma}_v(t) \end{aligned} \quad (24)$$

Without risking an abuse of notation, the time symbol  $t$  is omitted in the following covariance matrix for  $\mathbf{x}(t)$ , that is,

$$\begin{aligned}\Sigma_x(t) &= \text{Cov}(\mathbf{x}(t)) = \mathbb{E}\left(\left(\mathbf{x} - \mathbb{E}(\mathbf{x})\right)\left(\mathbf{x} - \mathbb{E}(\mathbf{x})\right)^\top\right) \\ &= \mathbb{E}\left(\tilde{\mathbf{x}}\tilde{\mathbf{x}}^\top + \hat{\mathbf{x}}\hat{\mathbf{x}}^\top\right) = \mathbf{P}(t) + \Sigma_{\hat{\mathbf{x}}}(t)\end{aligned}\quad (25)$$

where  $\tilde{\mathbf{x}} = \mathbf{x} - \hat{\mathbf{x}}$  is the state-estimate error. The second-to-last equality comes from the fact that the Kalman filter is unbiased and the state estimate is orthogonal to the estimate error (Drécourt, et al., 2006), that is

$$\mathbb{E}(\hat{\mathbf{x}}) = \mathbf{x}, \mathbb{E}(\tilde{\mathbf{x}}\hat{\mathbf{x}}^\top) = 0 \quad (26)$$

Substituting (25) into (24) gives

$$\Sigma_y(t) = \mathbf{C}\mathbf{P}(t)\mathbf{C}^\top + \mathbf{C}\Sigma_{\tilde{\mathbf{x}}}(t)\mathbf{C}^\top + \Sigma_v(t) \quad (27)$$

This completes the proof of Lemma 1. Q.E.D.

**Theorem 1:** *Given the dynamic system (17), the variance of the Kalman-filter-based residual generated by (18) to (22) is no larger than that of the correlation-based residual that does not consider any system dynamics, that is,*

$$\Sigma_{r,dynamic} \preceq \Sigma_{r,static} \quad (28)$$

**Proof:** From Section 3.2, the variance of the Kalman-filter-based residual is

$$\begin{aligned}\Sigma_{r,dynamic} &= \mathbb{E}\left(\left(\mathbf{y}(t) - \hat{\mathbf{y}}(t)\right)\left(\mathbf{y}(t) - \hat{\mathbf{y}}(t)\right)^\top\right) \\ &= \mathbf{C}\mathbf{P}(t)\mathbf{C}^\top + \Sigma_v(t)\end{aligned}\quad (29)$$

If we consider the output samples as independently distributed and do not take the system dynamics into account, the nominal estimation of system outputs is its expectation. Then, the covariance matrix of the residual is

$$\Sigma_{r,static} = \mathbb{E}\left(\left(\mathbf{y} - \mathbb{E}(\mathbf{y})\right)\left(\mathbf{y} - \mathbb{E}(\mathbf{y})\right)^\top\right) = \Sigma_y \quad (30)$$

Recalling (23) in Lemma 1, it follows that

$$\Sigma_{r,static} = \Sigma_{r,dynamic} + \mathbf{C}\Sigma_{\tilde{\mathbf{x}}}(t)\mathbf{C}^\top \quad (31)$$

Since the covariance matrix  $\Sigma_{\tilde{\mathbf{x}}}(t)$  is positive semidefinite, it is clear that (28) holds. Q.E.D.

Theorem 1 implies that considering system dynamics when generating residuals will reduce uncertainty in the resulting residual signal, thereby shrinking the deemed-normal region. Furthermore, (31) shows that the reduction in residual uncertainty corresponds exactly to the variance of the state prediction, which reflects the model's predictive ability.

### 3.4 Improving Fault Detection by Shrinking the Uncertainty

Although it has been shown that dynamic modelling shrinks the deemed-normal region, the question remains as to how it affects fault detection.

**Theorem 2:** *For optimal fault detection (16) based on the residual of the form (14), reducing residual uncertainty will improve fault detection, namely, increase the FDR without changing the FAR.*

**Proof:** As was noted in Section 3.1,  $J_{th}$  in the optimal solution (16) corresponds to the boundary of the normal region in the fault-free case. The value  $J_{th} = \chi^2(m, \alpha)$  depends on the degrees of freedom  $m$  and the predefined tolerance  $\alpha$  for FAR. Hence, the uncertainty (equivalent to variance for Gaussian distributions) in the residual does not affect  $J_{th}$ .

In the fault-free case, *i.e.*,  $\mathbf{f} = 0$ , the residual (14) is reduced to  $\boldsymbol{\varepsilon}$ , which comes from a centred Gaussian distribution. Then, the optimal statistics  $J$  given by (16) follows a  $\chi^2$ -distribution, whose only parameter is the degrees of freedom  $m$ , that is,

$$\mathbf{r} = \boldsymbol{\varepsilon} \sim \mathcal{N}(\mathbf{0}, \Sigma) \Rightarrow J = \mathbf{r}^\top \Sigma^{-1} \mathbf{r} \sim \chi^2(m) \quad (32)$$

Hence, FAR, as defined in (3), will be not affected by the uncertainty in the residual.

In the faulty case, *i.e.*,  $\mathbf{f} \neq 0$ , the expectation of the residual (14) is  $\mathbf{E}\mathbf{f}$ . Then, the distribution of the  $J$ -statistic becomes a noncentral  $\chi^2$ -distribution, that is,

$$\mathbf{r} \sim \mathcal{N}(\mathbf{E}\mathbf{f}, \Sigma) \Rightarrow J = \mathbf{r}^\top \Sigma^{-1} \mathbf{r} \sim \chi^2(m, \lambda) \quad (33)$$

where  $\lambda$  is the noncentrality parameter that is defined as

$$\lambda = \mathbf{f}^\top \mathbf{E}^\top \Sigma^{-1} \mathbf{E} \mathbf{f} \quad (34)$$

From Theorem 1, it follows that

$$\lambda_d = \mathbf{f}^\top \mathbf{E}^\top \Sigma_{r,dynamic}^{-1} \mathbf{E} \mathbf{f} \geq \lambda_s = \mathbf{f}^\top \mathbf{E}^\top \Sigma_{r,static}^{-1} \mathbf{E} \mathbf{f} \quad (35)$$

where  $\lambda_d$  and  $\lambda_s$  are the noncentrality parameters of  $J_d \sim \chi^2(m, \lambda_d)$  and  $J_s \sim \chi^2(m, \lambda_s)$ , respectively,  $J_d$  is the detection statistic of the Kalman-filter-based method, and  $J_s$  is that of static-correlation-based method. Since the noncentral  $\chi^2$ -distribution increases stochastically in the noncentrality parameter (Van der Vaart, 2000), it follows that

$$\Pr\{J_d > J_{th}\} \geq \Pr\{J_s > J_{th}\}, \forall J_{th} > 0 \quad (36)$$

This shows that the FDR of Kalman-filter-based method is no smaller than that of the static-correlation-based one. Q.E.D.

## 4. CASE STUDY

In this section, two faults are deliberately introduced into a simulated three-tank system to verify the theoretic results.

### 4.1 A Simulated Three-Tank System

As shown in Figure 1, the system consists of three tanks connected by pipes and two pumps to feed water into Tanks 1 and 2. Considering potential faults, the linearised model is

$$\begin{cases} \mathbf{x}(t+1) = \mathbf{A}\mathbf{x}(t) + \mathbf{B}\mathbf{u}(t) + \mathbf{B}_d\boldsymbol{\omega}(t) + \mathbf{B}_f\mathbf{f}(t) \\ \mathbf{y}(t) = \mathbf{C}\mathbf{x}(t) + \mathbf{D}\mathbf{u}(t) + \mathbf{D}_d\mathbf{v}(t) + \mathbf{D}_f\mathbf{f}(t) \end{cases} \quad (37)$$

where the system inputs  $\mathbf{u}(t) = [Q_1 \ Q_2]^\top = [\sin(t/2) + 0.5 \cos(t)]^\top$  are pump inlet flow rates, the system states  $\mathbf{x}(t)$  and outputs  $\mathbf{y}(t)$  are the vector  $[h_1 \ h_2 \ h_3]^\top$  consisting of the liquid levels in the three tanks, the noise is  $\boldsymbol{\omega}(t) \sim \mathcal{N}(0, 0.04\mathbf{I})$  and  $\mathbf{v}(t) \sim \mathcal{N}(0, 0.5\mathbf{I})$ , and the system matrices are

$$\mathbf{A} = \begin{bmatrix} 0.95 & 0 & 0 \\ 0.05 & 0.9 & 0 \\ 0 & 0.1 & 0.85 \end{bmatrix}, \mathbf{B} = \begin{bmatrix} 1 & 0 \\ 0 & 1 \\ 0 & 0 \end{bmatrix},$$

$$\mathbf{B}_f = \begin{bmatrix} 1 & 0 & 0 & 0 & 0 & 0 \\ 0 & 1 & 0 & 0 & 0 & 0 \\ 0 & 0 & 1 & 0 & 0 & 0 \end{bmatrix}, \mathbf{D}_f = \begin{bmatrix} 0 & 0 & 0 & 1 & 0 & 0 \\ 0 & 0 & 0 & 0 & 1 & 0 \\ 0 & 0 & 0 & 0 & 0 & 1 \end{bmatrix},$$

$$\mathbf{B}_d = \mathbf{D}_d = \mathbf{C} = \mathbf{I}, \mathbf{D} = 0$$

Two faulty scenarios are introduced: sensor bias in  $h_1$

$$\mathbf{f}(t) = [0 \ 0 \ 0 \ 5 \ 0 \ 0]^\top, t \in [600, 800]$$

and leakage in Tank 1

$$\mathbf{f}(t) = [-1 \ 0 \ 0 \ 0 \ 0 \ 0]^\top, t \in [600, 800]$$

The initial states are  $\mathbf{x}(t) = [20 \ 15 \ 10]^\top$ .

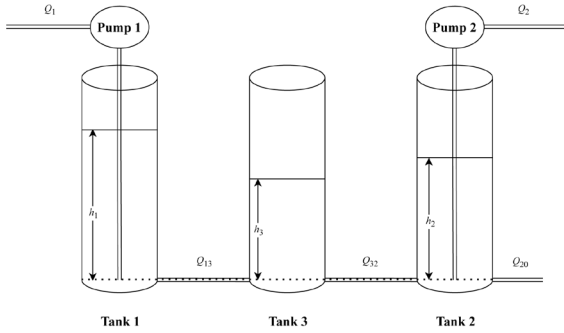


Figure 1. Diagram of a three-tank system

#### 4.2 Deemed-Normal Regions and Fault-Detection Results

Figure 2 shows the deemed-normal ellipsoids of a confidence of 0.68 (one standard deviation) for the three-tank system, according to Kalman-filter-based and static-correlation-based methods. The equations of the ellipsoids are

$$\mathbf{J} = \mathbf{r}^\top \boldsymbol{\Sigma}_{r,dynamic}^{-1} \mathbf{r} \leq 1 \text{ and } \mathbf{J} = \mathbf{r}^\top \boldsymbol{\Sigma}_{r,static}^{-1} \mathbf{r} \leq 1 \quad (38)$$

where the semi-axes lengths are  $[0.63, 0.61, 0.60]$  and  $[3.19, 2.56, 0.69]$  for Kalman-filter-based and static-correlation-based ellipsoids, respectively. It is clear that including system dynamics causes a large decrease in the uncertainty ellipsoid.

This subsection also presents the results of fault detection for the two faults at a confidence level of  $1 - \alpha = 0.99$ . For the sensor-bias fault, Figure 3 shows that the Kalman-filter-based method responds to the introduction and clearing of the fault much faster than the static-correlation-based one, as shown by the red arrows. Furthermore, the Kalman filter effectively tracks normal transient dynamics of the initial stage of the

simulation, thus preventing false alarms. In contrast, the static-correlation-based method raises false alarms in this area as shown by the red circle. For the leakage fault shown in Figure 4, the Kalman-filter-based method gives a clearer detection with a much higher detection rate. Compared with the first fault, this fault disturbs the dynamic behaviour of the system. Since the static-correlation-based method cannot model the dynamics, it has even worse results than for the first fault. The FDR and FAR are shown in Table 1. Notably, the FAR of the static method can exceed the tolerance of 1%. This is because of a mismatch between the modelling assumption and the system reality, which causes a violation of the stated tolerance for the FAR. On the other hand, the dynamic method maintains a FAR below 1%, which is attributed to the conservatism nature of the robust formulation (6).

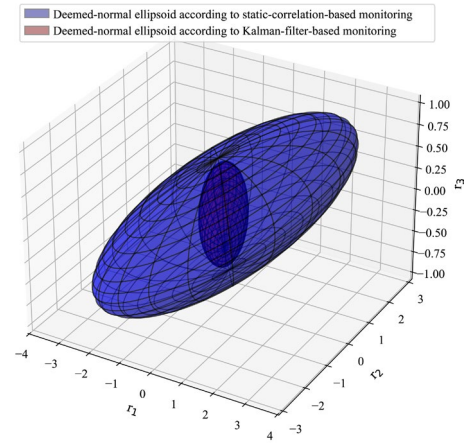


Figure 2. Deemed-normal ellipsoids ( $\alpha = 0.32$ ) of the three-tank system according to the (inside) Kalman-filter-based and (outside) static-correlation-based monitoring

Table 1. Fault-detection performance

	Leakage		Sensor bias	
	FDR	FAR	FDR	FAR
Static method	96%	7.38%	56%	0.88%
Dynamic method	99%	0.75%	100%	0.63%

## 5. CONCLUSIONS

This paper formulates a unified optimisation problem for fault detection based on hypothesis testing. The resulting optimal solution defines the deemed-normal region of the system. It is proven that dynamic information shrinks the deemed-normal region and improves detection performance in Gaussian LTI systems. The theoretical results are verified on a simulated three-tank system.

With these results, the paper provides a foundation for understanding fault detection in a simple case, *i.e.*, for Gaussian LTI systems and how dynamic information improves fault detection. This rigorous justification provides a roadmap towards advanced methods for more complex cases. For instance, having shown in this paper that eliminating model mismatch in Gaussian LTI systems shrinks the deemed-normal region and improves fault detection, what if a system is nonlinear, time-varying, non-Gaussian, or with

an ambiguous disturbance? How does removing model mismatch in these situations shrink the deemed-normal region and improve the detection performance? In addition, analysis including the idea of a deemed-normal region presented in this paper has the potential to be extended to a meaningful framework for performance assessment of fault diagnosis and fault-tolerant control systems.

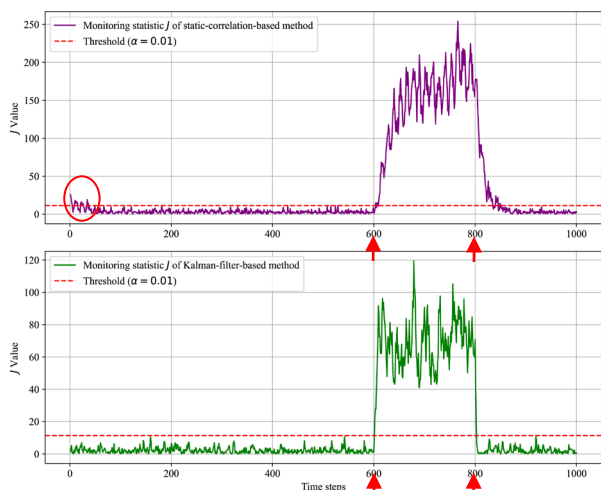


Figure 3. Monitoring results of a sensor bias in  $h_1$

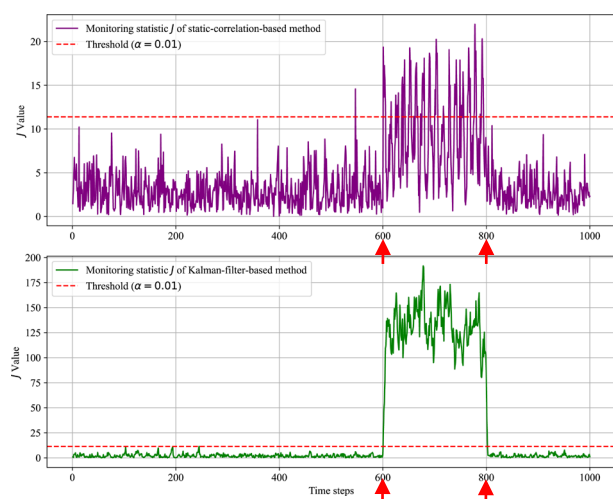


Figure 4. Monitoring results of a leakage in Tank 1

## REFERENCES

- Beard, R. V. (1971). *Failure accommodation in linear systems through self-reorganization*. [Doctoral dissertation]. Massachusetts Institute of Technology.
- Bernardi, E., & Adam, E. J. (2020). Observer-based fault detection and diagnosis strategy for industrial processes. *Journal of the Franklin Institute*, 357(14), 10054-10081.
- Ding, S. X. (2013). *Model-Based Fault Diagnosis Techniques: Design Schemes, Algorithms and Tools (2nd ed.)*. Springer Science & Business Media.
- Ding, S. X. (2021). *Advanced methods for fault diagnosis and fault-tolerant control*. Springer Berlin Heidelberg.
- Drécourt, J.-P., Madsen, M., & Rosbjerg, D. (2006). Bias aware Kalman filters: Comparison and improvements. *Advances in water resources*, 29(5), 77-718.
- Esfahani, P. M., & Lygeros, J. (2015). A tractable fault detection and isolation approach for nonlinear systems with probabilistic performance. *IEEE Transactions on Automatic Control*, 61(3), 633-647.
- Frank, F. M., & Ding, X. (1997). Survey of robust residual generation and evaluation methods in observer-based fault detection systems. *Journal of process control*, 7(6), 403-424.
- Gao, X., & Shardt, Y. A. (2021). Dynamic system modelling and process monitoring based on long-term dependency slow feature analysis. *Journal of Process Control*, 105, 27-47.
- Gao, X., Xie, J., & Shardt, Y. A. (2023). Concurrent Monitoring and Isolation of Static Deviations and Dynamic Anomalies with a Sparsity Constraint. *IFAC-PapersOnLine*, 56(2), pp. 11790-11795.
- Gao, X., Yang, F., & Feng, E. (2020). A process fault diagnosis method using multi-time scale dynamic feature extraction based on convolutional neural network. *The Canadian Journal of Chemical Engineering*, 98(6), 1280-1292.
- Gustafsson, F. (2000). *Adaptive filtering and change detection*. Chichester: John Wiley and Sons, LTD.
- Harmouche, J., Delpha, C., & Diallo, D. (2014). Incipient fault detection and diagnosis based on Kullback–Leibler divergence using principal component analysis: Part I. *Signal processing*, 94, 278-287.
- Jones, H. L. (1973). *Failure detection in linear systems*. [Doctoral dissertation]. Massachusetts Institute of Technology.
- Kalman, E. R. (1960). A new approach to linear filtering and prediction problems. *ASME Journal of Basic Engineering*, 82(1), 35-45.
- Khodarahmi, M., & Maihami, M. (2023). A review on Kalman filter models. *Archives of Computational Methods in Engineering*, 30(1), 727-747.
- Lee, J. M., Qin, J. S., & Lee, I. B. (2006). Fault detection and diagnosis based on modified independent component analysis. *AIChE journal*, 52(10), 3501-3514.
- Md Nor, M., Che Hassan, C., & Hussain, M. (2020). A review of data-driven fault detection and diagnosis methods: Applications in chemical process systems. *Reviews in Chemical Engineering*, 36(4), 513-553.
- Shang, C., Ding, S. X., & Ye, H. (2021). Distributionally robust fault detection design and assessment for dynamical systems. *Automatica*, 125, 109434.
- Shardt, Y. A. (2022). *Statistics for Chemical and Process Engineers: A Modern Approach (2nd ed.)*. Springer International Publishing.
- Song, Y., Zhong, M., Xue, T., Ding, S. X., & Li, W. (2020). Parity space-based fault isolation using minimum error minimax probability machine. *Control Engineering Practice*, 95, 104242.
- Van der Vaart, A. W. (2000). *Asymptotic statistics*. Cambridge university press.
- Wise, B. M., Ricker, N. L., Veltkamp, D. F., & Kowalski, B. R. (1990). A theoretical basis for the use of principal component models for monitoring multivariate processes. *Process control and quality*, 1(1), 41-51.